Cooperative Mechanism in the Homodimeric Myoglobin from *Nassa mutabilis*†

Massimo Coletta,*,‡ Paolo Ascenzi,§ Francesca Polizio,|| Giulietta Smulevich,⊥ Rosanna del Gaudio,# Marina Piscopo,# and Giuseppe Geraci#

Department of Experimental Medicine and Biochemical Sciences, University of Roma Tor Vergata, Via di Tor Vergata 135, 00133 Roma, Italy, Department of Biology, Third University of Roma, Viale G. Marconi 446, 00146 Roma, Italy, INFM and Department of Biology, University of Roma Tor Vergata, Viale della Ricerca Scientifica, 00133 Roma, Italy, Department of Chemistry, University of Firenze, Via Gino Capponi 9, 50121 Firenze, Italy, and Department of Genetics, General and Molecular Biology, University of Napoli, Via Mezzocannone 8, 80134 Napoli, Italy

Received June 9, 1997; Revised Manuscript Received December 8, 1997

ABSTRACT: Oxygen binding and spectroscopic properties of the homodimeric myoglobin (Mb) from the prosobranchia sea snail *Nassa mutabilis* have been investigated. Oxygen equilibrium curves are pH-independent and cooperative with $P_{50} = 5 \pm 1$ mmHg and $n \approx 1.5$. Circular dichroism spectra of the oxygenated and deoxygenated form of *N. mutabilis* Mb are superimposable between 190 and 250 nm, suggesting a mechanism for cooperative ligand binding that does not involve changes in the α-helical content of the whole protein. The oxygen dissociation process is biphasic and pH-dependent, with different pK_a values (=6.7 ± 0.2 and 8.5 ± 0.3) for the two phases. Moreover, the activation energy is essentially the same for both oxygen dissociation processes ($E_a = 56.4 \pm 2.1$ kJ/mol for the fast phase, and $E_a = 53.8 \pm 1.9$ kJ/mol for the slow phase), indicating that the rate difference for O_2 dissociation between the diliganded and the monoliganded species is mostly dependent on a variation of the activation entropy. Ferrous nitrosylated *N. mutabilis* Mb shows, at alkaline and neutral pH, axial and rhombic X-band EPR signals, respectively, which display below pH 6 a three-hyperfine pattern typical of five-coordination. The results presented here suggest that in *N. mutabilis* Mb the kinetic control of cooperativity operates through a mechanism never observed before in other hemoproteins, which requires a ligand-linked large enhancement for the value of the oxygen association process in a molecule not undergoing changes in quaternary structure.

In some species of gastropod sea snails of the prosobranchia subclass, namely *Buccinum undatum L.*, *Busycon canaliculatum*, *Cherithidea rhizophorarum*, and *Nassa mutabilis*, the presence of homodimeric myoglobin in the muscle cells has been reported (Bonner & Larsen, 1977; Geraci et al., 1977; Takagi et al., 1983). Such proteins are generally characterized by an essentially non cooperative oxygen binding behavior, except for *N. mutabilis* and *Buccinum undatum L.* Mb (Geraci et al., 1977; Terwilliger & Terwilliger, 1985). These are the only examples known as yet of cooperative Mb, while the occurrence of cooperative homodimeric Hb has been reported in the red blood cells of clams from the arcid family, such as *Anadania broughtonii*, *Scapharca inaequivalvis*, and *Noetia ponderosa* (Furuta et al., 1977; San George & Nagel, 1985; Chiancone et al., 1990).

In the present paper, we report for the first time a detailed characterization of the functional and spectroscopic properties of the cooperative homodimeric *N. mutabilis* Mb. These results have been analyzed in parallel with those of the *S. inaequivalvis* homodimeric Hb (Chiancone et al., 1990), whose X-ray crystal structure has been solved (Royer, 1994). Thus, the analysis of three-dimensional structures of deoxygenated and liganded forms of *S. inaequivalvis* have unravelled a peculiar mode of subunit assembly and of cooperative interaction operative in this homodimeric Hb, which involves a direct heme−heme communication (Royer, 1994). Such features appear to be responsible for an unusual pH-dependence of ligand binding kinetics observed in *S. inaequivalvis* (Coletta et al., 1990), and the same behavior has been reported for *N. mutabilis* Mb (Coletta et al., 1992), suggesting possible functional and structural similarities between the two hemoproteins. Therefore, the characterization of the cooperative mechanism in *N. mutabilis* Mb should define functional similarities and differences with respect to *S. inaequivalvis* homodimeric Hb. Present results have identified a new mechanism for the known expression of cooperativity in hemoproteins.

MATERIALS AND METHODS

N. mutabilis Mb was prepared from the radular muscles of the snail as previously reported (Geraci et al., 1977). The Mb preparation was gel filtered through a Sephadex G-100 column (Pharmacia, Uppsala, Sweden), showing a single band with an elution volume corresponding to the expected

† The financial support of the Ministero dell'Universita' e della Ricerca Scientifica e Tecnologica (MURST 40%) and of the Consiglio Nazionale delle Ricerche (CNR) is gratefully acknowledged.

* Author to whom all correspondence should be addressed. Telephone: 39+6+72596365. Fax: 39+6+72596353. E-mail: coletta@seneca.ccd.utovrm.it.

‡ Department of Experimental Medicine and Biochemical Sciences, University of Roma Tor Vergata.

§ Third University of Roma.

|| INFM and Department of Biology, University of Roma Tor Vergata.

⊥ University of Firenze.

University of Napoli.

[1] Abbreviations: Mb, myoglobin; Hb, hemoglobin; *N. mutabilis*, *Nassa mutabilis*; *S. inaequivalvis*, *Scapharca inaequivalvis*.

S0006-2960(97)01361-5 CCC: $15.00
Published on Web 02/13/1998

dimer molecular mass of 27 kDa (Geraci et al., 1977). All experiments have been carried out on such samples, and no evidence of monomer formation has ever been detected under the experimental conditions employed. The nitrosylated ferrous derivative of *N. mutabilis* Mb was prepared, as previously reported for sperm whale and horse heart Mbs (Ascenzi et al., 1985), by sequential addition of sodium dithionite (20 mg/mL final concentration) and of sodium nitrite (5 mg/mL final concentration) to the degassed Mb solution. The solutions were rapidly frozen at 100 K before the EPR spectrum was recorded. In this way, it is known that the equilibrium situation of MbNO observed by EPR at 100 K corresponds to that at 20 °C (Ascenzi et al., 1985).

Oxygen equilibrium experiments were carried out at 20 °C, using a Varian Dms-100 spectrophotometer. A small volume (≈3 mL) of degassed ferrous *N. mutabilis* Mb solution (≅30 μM heme) was kept in a large volume tonometer (≈600 mL of gas phase) with a cuvette fitted at the bottom for optical measurements of the protein solution, and with a lateral rubber septum to inject desired amounts of air in order to attain partial O_2 pressures inside the tonometer (Cirotto & Geraci, 1975).

Kinetic experiments were carried out between 8 and 35 °C using a Gibson-Durrum stopped-flow apparatus equipped with a 2 cm path length observation cell and linked to a computer-controlled data acquisition system (On Line Instrument Systems, Jefferson, GA). Two different types of kinetic experiments were performed to study the influence of possible alternative equilibrium conformations. (1) Deoxygenated Mb was prepared by flowing humidified Ar over the MbO_2 solution in a tonometer, with gentle shaking until the absorption spectrum was that of deoxyMb. This solution was mixed in a gastight syringe with different volumes of oxygenated buffer in order to obtain a Mb solution equilibrated at different levels of oxygen saturation. The O_2 dissociation kinetics was studied by mixing in the stopped-flow apparatus fully and partially O_2-saturated Mb solutions with sodium dithionite, and following spectroscopically the progress curves. (2) O_2 pulse experiments were performed, in which a solution of unliganded Mb in the presence of sodium dithionite was mixed in the stopped-flow apparatus with buffer equilibrated at different O_2 pressures (Gibson, 1973). Under these conditions, deoxyMb can initially bind O_2 very quickly, competing with sodium dithionite, reaching various degrees of ligand saturation, which depend on the oxygen pressure in the buffer solution and on the sodium dithionite concentration. The observed kinetics of O_2 dissociation corresponds to that of Mb molecules that have dynamically reached different degrees of oxygen saturation.

Circular dichroism spectra were obtained at 20 °C using a JASCO J500 spectropolarimeter.

X-band EPR spectra were recorded on a BRUKER ESP 300 spectrometer between 100 and 220 K.

All data were obtained in 0.1 M MES or potassium phosphate buffer (between pH 5.0 and 7.0), in 0.1 M Hepes buffer (between pH 6.7 and 8.0), and in 0.1 M Tris/HCl buffer (between pH 7.6 and 9.5).

RESULTS AND DISCUSSION

The equilibrium oxygen binding curve of *N. mutabilis* Mb is characterized by a sigmoidal shape with $P_{50} = 5 \pm 1$ mmHg and $n \approx 1.5$ (see Figure 1), a fairly high value considering that the molecule is a dimer (Geraci et al., 1977). Such behavior is pH-independent between pH 6.0 and 8.8 (see Figure 1), indicating that no ligand-linked proton uptake or release occurs. The thermodynamic analysis of the oxygen binding equilibrium properties for the cooperative homodimeric *N. mutabilis* can be made employing only two parameters, according to the phenomenological Adair mechanism (Adair, 1925). This rules out the usefulness of applying the two-state allosteric model, which implies instead the use of at least three parameters (Monod et al., 1965).

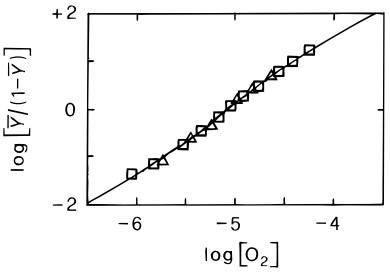

FIGURE 1: Isotherms of O_2 binding to *N. mutabilis* Mb at pH 6.0 (□, 0.1 M phosphate buffer) and pH 8.8 (△, 0.1 M Tris/HCl), when $T = 20$ °C. For the sake of clarity, superimposable experimental data at intermediate pH values have been omitted. The continuous line was calculated according to eq 1, with parameters reported in Table 1. [O_2] represents the concentration of the free ligand. For further details, see text.

A quaternary ligand-linked structural change can be followed by circular dichroism spectra of the oxygenated and deoxygenated forms in the far-UV region (i.e., between 190 and 250 nm). However, spectra for *N. mutabilis* Mb do not show any difference between the deoxygenated and oxygenated forms, suggesting that ligand binding is not associated with a variation of secondary structure of the dimer (see Figure 2A). On the other hand, ligand-linked effects are clearly present in the Soret region (between 390 and 480 nm) and in the region of the absorption of amino acid side chains (i.e., between 270 and 450 nm). These data suggest the alteration of the amino acid side chains interactions upon ligand binding and a strong effect on the geometry of the heme environment. Indeed, the θ_M value changes by a factor of about 4 during the transition between the unliganded and the liganded form (see Figure 2B,C). Interestingly, the ellipticity of the CD spectra of *N. mutabilis* Mb in the Soret region is negative (see Figure 2C), as also reported in the case of the common marine blood-worm *G. dibranchiata* Hb (Santucci et al., 1988), where the negative ellipticity has been attributed to an unusual heme orientation with respect to PheCD1 (Cooke & Wright, 1987; Arents & Love, 1989). Hence, it appears that ligand binding strongly affects this parameter together with alterations of some of the amino acid side chains. A similar situation, i.e., an invariance of the quaternary structure upon ligand binding, has also been reported for *S. inaequivalvis* Hb (Royer, 1994).

To have a better insight on the cooperative mechanism operative in *N. mutabilis* Mb, we have carried out two types of kinetic experiments. In one, kinetics of O_2 dissociation was studied on solutions of fully or partially oxygenated dimers. In this case, the results provide information on molecules that are in equilibrium with oxygen (Figure 3A). In the other case, the kinetics of oxygen dissociation was studied on dimers that were in the process of ligand binding,

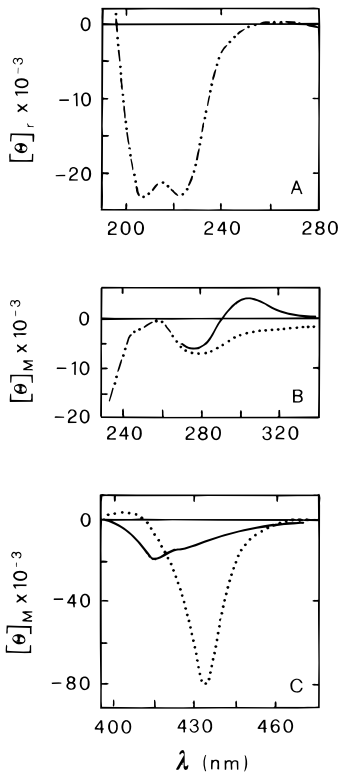

FIGURE 2: Circular dichroism spectra of oxygenated (continuous line) and deoxygenated (dotted line) Mb from *N. mutabilis*. Spectra are reported in different spectral regions, namely: (panel A) between 190 and 280 nm with ellipticity $[\theta]_r$ expressed as deg cm^2 dmol^{-1} of residue; (panel B) between 230 and 340 nm with ellipticity $[\theta]_M$ expressed as deg cm^2 dmol^{-1} of heme; (panel C) between 390 and 480 nm with ellipticity $[\theta]_M$ expressed as deg cm^2 dmol^{-1} of heme. Wherever the two spectra of the deoxygenated and oxygenated forms are superimposable, only one spectrum is reported as a dashed and dotted line (— ••). For further details, see text.

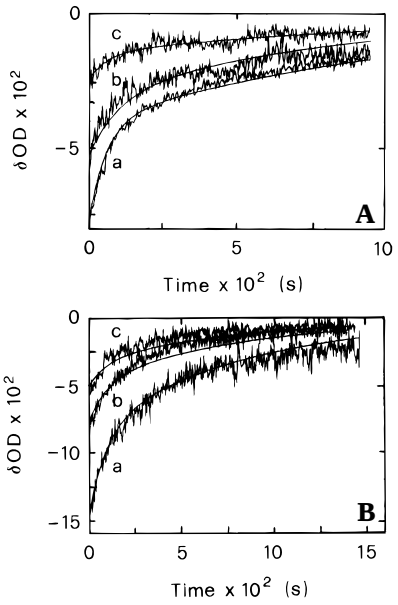

FIGURE 3: (panel A) Kinetics of O_2 dissociation from fully (curve a, $\bar{Y} = 1$) and partially oxygenated (curves b, $\bar{Y} = 0.66$; and curve c, $\bar{Y} = 0.31$) *N. mutabilis* Mb at pH 7.0 (0.1 M phosphate), when T = 20 °C and λ = 434 nm. Continuous lines were calculated according to Scheme 1. (panel B) O_2 pulse to *N. mutabilis* deoxyMb at pH 7.0 (0.1 M phosphate), when T = 20 °C and λ = 434 nm. Different concentrations of oxygen were employed in the different curves, attaining a different ligand saturation degree (i.e., $\bar{Y} = 1.0$ for curve a, $\bar{Y} = 0.65$ for curve b, and $\bar{Y} = 0.41$ for curve c). For further details, see text.

before establishing possible slow equilibrium conditions (Figure 3B). As already observed for the oxygen equilibrium binding studies (Figure 1), the results of the oxygen dissociation kinetics (Figure 3) cannot be accounted for by a two-state allosteric model (Monod et al., 1965). In fact, the results of both experiments of oxygen dissociation, from molecules equilibrated at different partial ligand saturations (Figure 3A) and from molecules which dynamically reached different oxygen saturation levels (Figure 3B), display biphasic patterns which cannot be due to an intrinsic kinetic subunit heterogeneity since the molecule is a homodimer. Therefore, the analysis of data in Figure 3 has been performed using the phenomenological Adair model (Adair, 1925) according to the following scheme, which is also valid for the equilibrium data reported in Figure 1

Scheme 1

$$\mathrm{Mb} + \mathrm{O_2} \underset{k^1_{off}}{\overset{k^1_{on}}{\rightleftharpoons}} \mathrm{Mb(O_2)_1} + \mathrm{O_2} \underset{k^2_{off}}{\overset{k^2_{on}}{\rightleftharpoons}} \mathrm{Mb(O_2)_2}$$

where K_1 ($=k^1_{on}/k^1_{off}$) is the equilibrium association constant for oxygen to the unliganded Mb dimer and K_2 ($=k^2_{on}/k^2_{off}$) is the equilibrium association constant for oxygen binding to the monoliganded $Mb(O_2)_1$ species. The ratio δ ($=K_2/K_1$) is a dimensionless factor which indicates the cooperative character of the ligand binding process, $\delta > 1$ reflecting the degree of enhancement of the oxygen affinity equilibrium constant for the second binding step, as a consequence of a ligand-linked structural change(s) taking place upon binding of the first O_2 molecule. The mechanism described in Scheme 1 implies that the dimer exists in two conformations (which we call conformations A and B). In the unliganded form the protein has conformation A, and the functional properties of the first binding step indeed refer to this conformation. To bind the second ligand the dimer must undergo a transition to conformation B. However, this transition in the monoliganded form does not relate to a quaternary structural variation of the whole dimer, as indicated by CD spectra (see Figure 2A), but instead to changes of the heme environment and of the conformation of some amino acid side chain(s) (see Figure 2B,C). Therefore, K_1 is the oxygen equilibrium affinity of the dimer in the conformation A, and K_2 is the ligand binding affinity in the conformation B. However, the scheme also implies that the conformational transition is allowed only in the monoliganded form. From this mechanism the following equation can be derived, which has been employed also for the analysis of data from *S. inaequivalvis* homodimeric Hb (Ikeda-Saito et al., 1983), and which is used here for the analysis of ligand binding isotherms of *N. mutabilis* Mb

$$\bar{Y} = K_1[\mathrm{O_2}](1 + K_2[\mathrm{O_2}])/[1 + K_1[\mathrm{O_2}](2 + K_2[\mathrm{O_2}])] \quad (1)$$

Since *N. mutabilis* Mb is a homodimer (Geraci et al., 1977; Parente et al., 1993), the biphasic kinetic pattern of O_2 dissociation from this Mb (see Figure 3) must be referred to a difference in the O_2 dissociation behavior between the diliganded (i.e., k^2_{off}) and the monoliganded species (i.e.,

Table 1: Thermodynamic and Kinetic Parameters for the O_2 Binding of *N. mutabilis* Mb in 0.1 M phosphate at pH 7.0 and 20 °C

equilibrium parameters	
K_1 (M^{-1})	3.2 (±0.4) × 10^4
δ (=K_2/K_1)	14 (±1.3)
kinetic parameters	
k^1_{on} (M^{-1} s^{-1})	3.0 × 10^5[a]
k^1_{off} (s^{-1})	9.2 (±1.1)
σ_{on} (=k^2_{on}/k^1_{on})	127[a]
σ_{off} (=k^2_{off}/k^1_{off})	9.1 (±0.7)

[a] Derived on the basis of the following relationships: $k^1_{on} = K_1 k^1_{off}$; $\sigma_{on} = \delta\sigma_{off}$.

k^1_{off}), which can be expressed by the factor σ_{off} (=k^2_{off}/k^1_{off}). The continuous lines shown as curves a in Figure 3A,B represent the least-squares fitting of the experimental curve according to Scheme 1, using the parameters reported in Table 1. The investigation on the oxygen dissociation kinetics has also been extended to partially saturated Mb in equilibrium with O_2 (see Figure 3A, curves b and c), and to partially saturated Mb that has dynamically achieved a partial saturation level (Figure 3B, curves b and c). The continuous curves in Figure 3 show that Scheme 1 and parameters reported in Table 1 are able to fully account for the cooperative behavior of *N. mutabilis* Mb also at intermediate saturation degrees. This observation unequivocally demonstrates that no slow conformational equilibria seem to be present in the ligand binding (or dissociation) dynamic pathway.

The kinetic heterogeneity for oxygen dissociation (see Figure 3) and the absence of a slow equilibration rate at intermediate ligand saturation levels (as from the O_2 pulse) can account for the cooperative character of equilibrium binding isotherms (see Figure 1) only if the kinetic control of the cooperative mechanism operates through a ligand-linked variation of the association rate constant. Thus, according to Scheme 1 at pH 7.0 a δ (=K_2/K_1) of 14 ± 2 [as required from the O_2 binding isotherms (see Figure 1 and Table 1)] and the kinetic biphasicity (see Table 1) with σ_{off} = 9.1 ± 0.7 demand altogether a dramatic increase in the association rate constant of *N. mutabilis* Mb during ligand binding given by σ_{on} (=$k^2_{on}/k^1_{on} = \delta\sigma_{off}$) = 127 (see Table 1). Therefore, equilibrium data reported in Figure 1 and dissociation kinetics reported in Figure 3 turn out to be perfectly compatible with each other, and no further complexity is needed with respect to Scheme 1 to quantitatively describe the cooperative mechanism of *N. mutabilis* Mb.

The mechanism described above for *N. mutabilis* Mb is the only one which can account in such a simple fashion for the whole set of data reported in Figures 1 and 3. However, it is drastically different from that operative in cooperative Hbs from mammals and fishes (Brunori et al., 1989) as well as in *S. inaequivalvis* Hb (Antonini et al., 1984), where the kinetic control of the cooperative mechanism for O_2 binding is exerted through a variation of the oxygen dissociation rate constant. It suggests that Mb and Hb may significantly vary in the kinetic control mechanisms of oxygen binding, indicating that in *N. mutabilis* Mb oxygen cooperative binding brings about a variation of the association rate constant, as for CO binding to hemoglobins (Brunori et al., 1989), and envisaging the possibility that, unlike Hbs, in this Mb molecule O_2 and CO cooperative binding are regulated in a similar fashion.

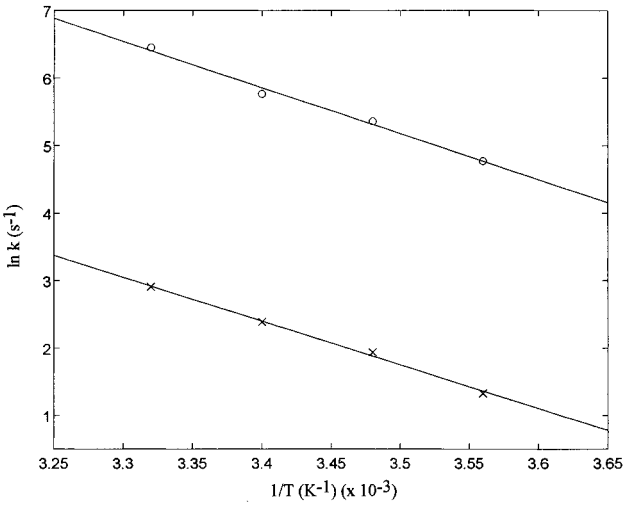

FIGURE 4: Arrhenius plot of the temperature dependence for the O_2 dissociation rate constant from *N. mutabilis* Mb for the fast (○) and the slow phase (×). Continuous lines correspond to the least-squares fitting to experimental data according to the following equation: ln k = ln $A - E_a/RT$ (eq 2). The following parameters have been obtained: for the fast phase, ln A = 29.0 ± 2.7 and E_a = 56.4 ± 3.1 kJ/mol; for the slow phase, ln A = 24.5 ± 2.2 and E_a = 53.8 ± 2.8 kJ/mol. For further details, see text.

The mechanism proposed for the kinetic control of cooperativity in *N. mutabilis* Mb is also able to account for previous observations, which revealed no increase of the ligand association rate constant during the ligation process (Geraci et al., 1976). Thus, on the basis of the thermodynamic and kinetic characterization (see Figures 1 and 3 and Table 1), the occurrence of $k^2_{on} \gg k^1_{on}$ (as from $\sigma_{on} \gg 1$, see Table 1) should impair the detection of a saturation-dependent increase of the observed ligand binding process because of an expected large predominance of diliganded molecules at every saturation degree $\bar{Y}$. It follows that, because of the large value of σ_{on} (=127, see Table 1), the overall association rate constant is dominated by the very fast association rate for the second binding step (k^2_{on}= 3.8 × 10^7 M^{-1} s^{-1}). Consequently, the cooperative mechanism predicts that, at intermediate ligand saturation degrees, O_2 molecules are not statistically distributed among the hemes of the homodimer and further requires the occurrence of a marked biphasicity for the O_2 dissociation process to compensate, at least partially, for the dramatic enhancement of the association rate constant. Under these conditions, it becomes obvious that a direct measurement of the O_2 binding kinetic process is not able to unravel any meaningful feature of the cooperative mechanism, since the expected behavior of the system could be phenomenologically described even with only one rate constant. Therefore, the crucial aspect for understanding the cooperative mechanism operative in *N. mutabilis* Mb depends on a detailed analysis of the O_2 dissociation kinetic process together with the equilibrium binding isotherms.

The temperature dependence of the O_2 dissociation process at pH 7.0 shows that the activation energy is essentially the same for both O_2 dissociation phases (E_a = 56.4 ± 2.1 kJ/mol for the fast phase, and E_a = 53.8 ± 1.9 kJ/mol for the slow phase, see Figure 4). It indicates that a difference in the activation entropy of the oxygen dissociation process from the fully oxygenated molecule ($\Delta S^{\ddagger}$ = − 27.1 ± 2.7 eu) and from the monoliganded species ($\Delta S^{\ddagger}$ = − 54.4 ±

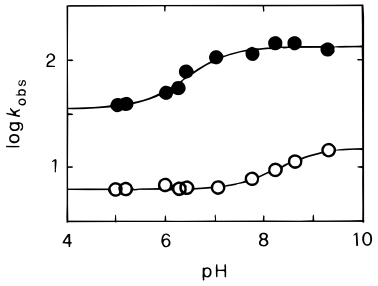

FIGURE 5: pH-dependence of the fast (●) and the slow (○) O_2 dissociation rate constant from fully oxygenated *N. mutabilis* Mb, when $T = 20$ °C and $\lambda = 434$ nm. The continuous line corresponds to the nonlinear least-squares fitting of the data according to the equation $k_{obs} = k_{alk}/(1 + K_a[H^+]) + k_{ac}K_a[H^+]/(1 + K_a[H^+])$ (eq 3) with the following set of parameters: $k_{alk} = 133.5 \pm 7.9\ s^{-1}$, $k_{ac} = 35.6 \pm 2.8\ s^{-1}$, and $K_a = 5.2\ (\pm 0.9) \times 10^6\ M^{-1}$ for the fast phase; $k_{alk} = 15.1 \pm 0.8\ s^{-1}$, $k_{ac} = 6.3 \pm 0.5\ s^{-1}$, and $K_a = 3.0\ (\pm 0.7) \times 10^8\ M^{-1}$ for the slow phase. For further details, see text.

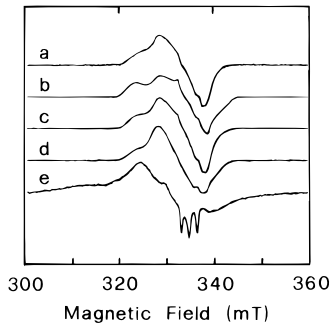

FIGURE 6: EPR spectra of nitrosylated *N. mutabilis* Mb at pH 8.7 in 0.1 M Tris/HCl and 100 K (spectrum a), at pH 7.0 in 0.1 M phosphate and 100 K (spectrum b), at pH 7.0 in 0.1 M Hepes and 100 K (spectrum c), at pH 7.0 in 0.1 M phosphate and 220 K (spectrum d), and at pH 5.6 in 0.1 M acetate and 100 K (spectrum e). Setting conditions: 9.42 GHz microwave frequency, 20 mW microwave power, 0.1 mT modulation amplitude. For further details, see text.

4.5 eu) can account for the rate difference of the biphasic progress curve (see Figure 3, curve a). Therefore, it appears that after the dissociation of the first O_2 molecule from the diliganded dimer, the transition in the monoliganded species from conformation B to A renders drastically more negative the entropy change for the formation of the activated complex during the dissociation of the second oxygen molecule, without altering significantly the enthalpic contribution. It clearly indicates that in *N. mutabilis* Mb cooperative ligand binding is a totally entropy-driven process, possibly related either to alterations of the number of water molecules present at the subunit interface, as in *S. inaequivalvis* Hb (Royer, 1994), or to a movement of a side chain, which alters the energy of conformational fluctuations responsible for the regulation of the dynamic outward pathway of the ligand (see below).

O_2 dissociation kinetics from fully oxygenated *N. mutabilis* Mb displays a pH-dependence (Figure 5), suggesting that the lack of a proton effect on equilibrium properties (see Figure 1) is related to a compensation between the ligand association and dissociation process. Thus, the absence of a proton-linked effect on the O_2 binding equilibrium properties simply means that the pK_a of functionally relevant residues is the same in the deoxygenated and in the oxygenated forms. Such a statement does not imply that the protonation of groups does not affect the oxygen dissociation or association rates, but it simply means that the pK_a is the same for the two processes. In other words, data reported in Figures 1 and 5 taken together show that O_2 binding to *N. mutabilis* Mb is regulated by changes in the protonation state of some residue(s), but this state is not different in the deoxy and oxy forms.

The pH-dependence appears very different for the two phases (see Figure 5), and, on the basis of the mechanism proposed above, the O_2 dissociation from the diliganded hemoprotein displays a p$K_a = 6.7 \pm 0.2$, which may be attributed to the protonation of the distal histidine. O_2 dissociation from the monoliganded species, following the ligand-linked structural change(s), displays a p$K_a = 8.5 \pm 0.3$ (see Figure 5). This feature can be accounted for in Scheme 1, since the lack of pH-dependence for the O_2 binding isotherms may be explained by assuming that in conformation B ligand binding is regulated by a group with a p$K_a = 6.7$, which is constant in the monoliganded and in the diliganded form. On the other hand, the switch to conformation A brings into play a new titratable group with a p$K_a = 8.5$, which has the same pK_a in the monoliganded and unliganded form of the protein. Therefore, there are two possible mechanisms consistent with these results. (i) The ligand-linked conformational change(s) from conformation B to A brings about a variation of the type of amino acid side chain group stabilizing the bound O_2, thus modulating the ligand dissociation process and its entropic contribution (see above), or else (ii) the pK_a value of an individual group varies upon the transition between conformation B and A in the monoliganded species, this being related to a proton-linked equilibrium between (at least) two different structural arrangements of the same protonating group. In the latter case, there should be a very fast structural transition between them.

The pH- and temperature-dependence of the kinetic properties of oxyMb from *N. mutabilis* find a counterpart in EPR spectroscopic changes of the ferrous nitrosylated form, which can give information for the structure of the diliganded dimer. At alkaline pH (=8.7) and 100 K an axial EPR signal is observed (Figure 6, spectrum a), as already reported for sperm whale and horse heart Mb (Ascenzi et al., 1985). Lowering the pH in 0.1 M phosphate buffer to pH 7.0 (at 100 K) brings about the appearance of a rhombic EPR signal (Figure 6, spectrum b), which is not observed if phosphate is replaced by Hepes (see Figure 6, spectrum c). No effect was observed by varying the chloride concentration in the absence of phosphate, and this observation indicates the occurrence of a phosphate-induced conformational transition, likely limiting the ligand rotational freedom (Bartnicki et al., 1983). The molecular mechanism responsible for this phenomenon is not unequivocally established, but it is reasonable to claim that it is probably related to the same phenomenon responsible for the entropy change reported above. This interpretation seems in line also with the observation that in raising the temperature from 100 to 220 K at pH 7.0 in 0.1 M phosphate buffer an axial EPR signal is recovered (see Figure 6, spectrum d), as also is observed for elephant Mb (Bartnicki et al., 1983). It is important to remark that such spectroscopic changes pertain to a ferrous liganded species of *N. mutabilis* Mb with a ligand (i.e., NO) which shares similar properties with the bound O_2; therefore,

these pH-dependent structural features might be referrable to the O_2-bound form as well.

Lowering pH below 6.0 induces the appearance of a three-line hyperfine pattern in the g_z region of the spectrum (Figure 6, spectrum e), which has been observed in all ferrous nitrosylated hemoproteins investigated (Perutz, 1979; Blumberg, 1981), and which has been suggested to reflect the cleavage, or severe weakening, of the proximal His−Fe bond (Ascenzi et al., 1985). As already reported for other hemoproteins (Ascenzi et al., 1985; Brunori et al., 1989; Coletta et al., 1990), the pK_a value of the pentacoordinate to hexacoordinate transition in ferrous nitrosylated homodimeric Mb (≈6.3) is higher than that reported for the penta- to the tetracoordinate form in the deoxyMb from *N. mutabilis* ([pK_a = 4.0 ± 0.2; see Coletta et al. (1992)]. It suggests that the presence of an axial ligand, such as NO, drastically decreases the energy of the proximal His−Fe bond.

The EPR spectra clearly indicate the occurrence of a different geometry at different pH values of the heme surroundings for the conformation B (see Figure 6). Furthermore, CD spectra, as well as kinetic and equilibrium properties, collectively suggest that cooperativity in *N. mutabilis* Mb is related to alterations of the heme environment and of the conformation of some amino acid side chains (see Figure 2B,C), even though the secondary structure of the protein does not seem to be significantly altered (see Figure 2A).

The present study indicates that *N. mutabilis* Mb has a kinetic behavior drastically different from that of the cooperative homodimeric Hb from *S. inaequivalvis* (Antonini et al., 1984), even though it displays some similar functional features such as the relatively low affinity for oxygen and cooperativity for ligand binding [see Chiancone et al. 1990)]. Indeed, the control of cooperativity in *N. mutabilis* Mb appears to be exerted mainly through the ligand-linked variation of the ligand association rate constant. In addition, the oxygen dissociation kinetic behavior is pH-dependent in *N. mutabilis* Mb, while it is not proton-linked in the homodimeric *S. inaequivalvis* Hb (Antonini et al., 1984). The different ligand binding mode indicates that the liganded forms (either oxygenated and/or nitrosylated) of the two homodimeric hemoproteins have significant structural and functional differences, as also suggested by comparative resonance Raman spectroscopic studies (Song et al., 1993; Smulevich et al., 1995).

In conclusion, the different expression of cooperativity for the two homodimeric hemoproteins from *N. mutabilis* and *S. inaequivalvis* clearly indicates the existence of multiple strategies for the realization of a cooperative mechanism, which might underlie the occurrence of parallel evolutionary processes leading to a similar but not identical functional result.

ACKNOWLEDGMENT

The authors thank Prof. A. Desideri for several fruitful discussions and Prof. M. Brunori for having made available the rapid-mixing instrument at the Department of Biochemical Sciences, University of Rome "La Sapienza".

REFERENCES

Adair, G. S. (1925) *J. Biol. Chem. 63*, 529−545.
Antonini, E., Ascoli, F., Brunori, M., Chiancone, E., Verzili, D., Morris, R. J., & Gibson, Q. H. (1984) *J. Biol. Chem. 259*, 6730−6738.
Arents, G., & Love, W. E. (1989) *J. Mol. Biol. 210*, 149−161.
Ascenzi, P., Coletta, M., Desideri, A., & Brunori, M. (1985) *Biochim. Biophys. Acta 829*, 299−302.
Bartnicki, D. E., Mizukami, H., & Romero-Herrera, A. E. (1983) *J. Biol. Chem. 258*, 1599−1602.
Blumberg, W. E. (1981) in *Hemoglobin* (Antonini, E., Rossi-Bernardi, L., & Chiancone, E., Eds.) *Methods in Enzymol. 76*, 312−329.
Bonner A., & Larsen R. A. (1977) *FEBS Lett. 73*, 201−203.
Brunori, M., Coletta, M., Ascenzi, P., & Bolognesi, M. (1989) *J. Mol. Liq. 42*, 175−193.
Chiancone, E., Verzili, D., Boffi, A., Royer, W. E., Jr., & Hendrickson, W. A. (1990) *Biophys. Chem. 37*, 287−292.
Cirotto, C., & Geraci, G. (1975) *Comp. Biochem. Physiol. 51A*, 159−163.
Coletta, M., Boffi, A., Ascenzi, P., Brunori, M., & Chiancone, E. (1990) *J. Biol. Chem. 265*, 4828−4830.
Coletta, M., Ascenzi, P., Smulevich, G., Mantini, A. R., Del Gaudio, R., Piscopo, M., & Geraci, G. (1992) *FEBS Lett 296*, 184−186.
Cooke, R. M., & Wright, P. E. (1987) *Eur. J. Biochem. 166*, 409−414.
Furuta, H., Ohe, M., & Kajita, A. (1977) *J. Biochem. 82*, 1723−1730.
Geraci, G., Parkhurst, L. J., Sada, A., & Cirotto, C. (1976) in *Myoglobins* (Schneck, A. G., & Van de Casserie, C., Eds.) pp 75−89, Universite' Libre de Bruxelles, Bruxelles.
Geraci, G., Sada, A., & Cirotto, C. (1977) *Eur. J. Biochem. 77*, 555−560.
Gibson, Q. H. (1973) *Proc. Natl. Acad. Sci. U.S.A. 70*, 1−4.
Ikeda-Saito, M., Yonetani, T., Chiancone, E., Ascoli, F., Verzili, D., & Antonini, E. (1983) *J. Mol. Biol. 170*, 1009−1018.
Monod, J., Wyman, J., & Changeux, J.-P. (1965) *J. Mol. Biol. 12*, 88−118.
Parente, A., Verde, C., Malorni, A., Montecucchi, P. C., Aniello, F., & Geraci, G. (1993) *Biochim. Biophys. Acta 1162*, 1−9.
Perutz, M. F. (1979) *Ann. Rev. Biochem. 48*, 327−386.
Royer, W. E., Jr. (1994) *J. Mol. Biol. 235*, 657−681.
San George, R. C., & Nagel, R. L. (1985) *J. Biol. Chem. 260*, 4331−4337.
Santucci, R., Mintorovitch, J., Constantinidis, I., Satterlee, J. D., & Ascoli, F. (1988) *Biochim. Biophys. Acta 953*, 201−204.
Smulevich, G., Mantini, A. R., Paoli, M., Coletta, M., & Geraci, G. (1995) *Biochemistry 34*, 7507−7516.
Song, S., Boffi, A., Chiancone, E., & Rousseau, D. L. (1993) *Biochemistry 32*, 6330−6336.
Takagi, T., Tobita, M., & Shikama, K. (1983) *Biochim. Biophys. Acta 745*, 32−36.
Terwilliger, R. C., & Terwilliger, N. B. (1985) *Comp. Biochem. Physiol. 81B*, 255−261.

BI9713613